

Trajectory elongation strategies with minimum curvature discontinuities for a Dubins vehicle

Aditya K. Rao, Twinkle Tripathy

Department of Electrical Engineering, Indian Institute of Technology Kanpur, Kanpur-208016, India

Abstract

In this paper, we present strategies for designing curvature-bounded trajectories of any desired length between any two given oriented points. The proposed trajectory is constructed by the concatenation of three circular arcs of varying radii. Such a trajectory guarantees a complete coverage of the maximum set of reachable lengths while minimising the number of changeover points in the trajectory to a maximum of two under all scenarios. Additionally, by using the notion of internally tangent circles, we expand the set of Circle-Circle-Circle trajectories to eight kinds, consisting of $\{LLL, LLR, LRR, LRL, RRL, RLL, RLR, RRR\}$ paths. The paper presents a mathematical formulation of the proposed trajectory and the conditions for the existence and classification of each kind of trajectory. We also analyse the variation of the length of the trajectory using suitable elongation strategies and derive the set of reachable lengths for all pairs of oriented points. Finally, the results of this paper are illustrated using numerical simulations.

Key words: Dubins Shortest Path, curvature bounded trajectories, elongation strategies, trajectory planning

1 Introduction

The problem of planning trajectories between two given points for an autonomous vehicle moving at a constant speed has been explored extensively in literature of guidance and control. It finds its applications in a variety of fields such as parking problems [1], warehouse automation [2], missile guidance [3], *etc.* The feasibility of such problems towards real world applications leads to additional requirements such as curvature-boundedness, desired lengths of the trajectories, directions of motion at initial and final points [4], and optimal energy consumption [5].

The shortest trajectory between any two oriented points in \mathbb{R}^2 is either of the form Circle-Circle-Circle (CCC) or Circle-Straight Line-Circle (CSC) ([6], [7]). This trajectory is called Dubins Shortest Path. A relaxed problem is to find trajectories of desired lengths between an oriented point and a fixed point in \mathbb{R}^2 . The shortest path in such a scenario is of the form Circle-Circle (CC) or Circle-Straight Line (CS) as shown in [8]. Elongation of certain subsections of such a minimum length trajectory is done to get trajectories of desired lengths. Without fixing the tangent vector at the final point, the authors in [4] and [9]

present multiple such elongation strategies. However, it is shown in [10] that between some initial oriented points and final points, there exist no curvature-bounded paths for a certain range of lengths. This classification of the set of reachable lengths is elaborated in [10] and elongation strategies are presented for all the cases.

The authors in [11] discuss elongation strategies achieved by increasing the radii of curvature of the terminal circles when the Dubins Shortest Path is of the form CSC. Alternatively, the authors in [12] propose replacing the straight-line segment with an elongated path. The use of clothoid arcs of arbitrary lengths is proposed in [13] for trajectory elongation while also ensuring a continuity in the curvature profile. The authors in [14] provide a comprehensive analysis of the set of reachable lengths given any two oriented points and propose elongation strategies for all pairs of oriented points. They also highlight the cases when certain lengths are not reachable for some pairs of oriented points. In [15], the Dubins Shortest Path is extended to three-dimensional space, followed by the introduction of trajectory elongation methods to attain any desired length. The authors in [16] analyse the set of reachable oriented points from any initial oriented point at time t_f for a Dubins vehicle with symmetric bounds on the control input. Further, in the case of asymmetric bounds on the control input, the set of reachable oriented points is derived in [17]. Note that, in general, the use of elongation based strategies increases the number of

* This work was not supported by any organisation.

Email addresses: adikrao@iitk.ac.in (Aditya K. Rao),
ttripathy@iitk.ac.in (Twinkle Tripathy).

changeover points. The strategies presented in [11–14] increase the number of changeover points by as large as six. To address this problem, in one of our earlier works [18], we propose to construct trajectories of desired lengths using exactly two circles of varying radius minimising the changeover points to exactly one always.

Geometrical curves other than circles and straight lines are also used in the literature to construct trajectories of desired lengths. The use of elliptical curves and Bezier curves is proposed in [19] and [20], respectively, to achieve trajectories of desired lengths. However, the use of geometrical curves, other than the circles and straight lines, limits the set of reachable lengths. Alternate methods have also been explored to achieve a trajectory of desired length between any two oriented points. The authors in [21] construct the trajectory as a polynomial expression and find its parameters that satisfy various constraints. Optimal control theory is employed in [22] and [23] to develop closed-form Impact Time Control Guidance (ITCG) laws, allowing a vehicle to manoeuvre between two oriented points with a fixed time of flight. In contrast, [24] introduces a structure-homotopy-based planner that generates trajectories by focusing on endpoint conditions rather than relying on elongation strategies.

In this work, we focus on planning trajectories of desired lengths between any two given oriented points while minimising the number of changeover points and ensuring the maximum coverage of the set of reachable lengths. The major contributions of this work are as follows:

- *Design of paths of desired lengths:* We propose to construct a feasible trajectory by concatenating three circles. We show that there always exist infinitely many such curvature-bounded trajectories of varying lengths between any two oriented points and present analytical results for the same.
- *Internally tangent trajectories:* The Circle-Circle-Circle Dubins paths are of form $\{RLR, LRL\}$ in literature. The proposed solution expands the Dubins path of form Circle-Circle-Circle (CCC) to eight forms, namely $\{LLL, LLR, LRR, LRL, RRL, RLL, RLR, RRR\}$, by considering circles that are internally tangent. We also show that the Circle-Circle trajectories of form $\{LL, LR, RR, RL\}$ presented in [18] emerge naturally as a subset of the proposed solution.
- *Set of reachable lengths:* We find the set of reachable lengths for these trajectories and show that it is equal to the maximum set of reachable lengths. Given a reachable length, we show that there exist multiple curvature-bounded trajectories of a desired length.
- *Reduction in the number of points of curvature discontinuity:* The proposed trajectory always has a maximum of two changeover points for any two arbitrarily oriented points and a given desired length. This minimisation is achieved without any reduction in the maximum set of reachable lengths.

The paper is organised as follows: Section 2 presents some preliminary technical results that are used subsequently in the paper. Section 3 presents the problem statement and describes the proposed method of trajectory design with the motivation behind it. Section 4 provides a mathematical description of the proposed Circle-Circle-Circle trajectory and the conditions necessary for its existence. Building on these results, Section 5 explores elongation strategies and their impact on the attributes of the proposed trajectories. Section 6 discusses the set of reachable lengths for various pairs of oriented points. Section 7 presents numerical simulations to illustrate the theoretical findings. Finally, Section 8 concludes the paper and suggests potential directions for future research.

2 Preliminaries and Notations

Trajectories constructed using circles have been utilised frequently in path planning problems. They provide simplicity in design and require constant lateral acceleration in physical implementation. We define a curvature-bounded trajectory as a function Λ and the minimum turn radius allowed for any such trajectory as r_{\min} .

Definition 1 Given two oriented points $A = (\mathbf{a}, \alpha)$ and $B = (\mathbf{b}, \beta)$, $\Lambda : [0, s] \rightarrow \mathbb{R}^2$ denotes a feasible curvature-bounded trajectory connecting the oriented points such that

- $\Lambda(t)$ is parameterized by arc length and is C^1 and piecewise C^2 .
- $|\Lambda'(t)| = 1 \forall t \in [0, s]$
- $\Lambda(0) = \mathbf{a}, \Lambda(s) = \mathbf{b}, \Lambda'(0) = (\cos \alpha, \sin \alpha), \Lambda'(s) = (\cos \beta, \sin \beta)$
- $\|\Lambda''(t)\| \leq 1/r_{\min}, t \in [0, s]$ when defined,

where $r_{\min} > 0$. The length of the trajectory is denoted by $l(\Lambda)$.

We define C_P^r and C_P^l as two tangential circles of radius r_{\min} at an oriented point P with their centres at \mathbf{c}_P^r and \mathbf{c}_P^l , respectively, as shown in Fig. 1. These circles correspond to a right turn (denoted by R) and a left turn (denoted by L) on a circular arc of radius r_{\min} . Further, we define the function $d : \mathbb{R}^2 \times \mathbb{R}^2 \rightarrow \mathbb{R}$ that gives the Euclidean distance between any two points in \mathbb{R}^2 plane.

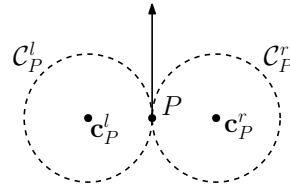


Fig. 1. Two circles C_P^r and C_P^l at oriented points P

The radius of a circle is generally a positive real number. However, we denote the radius of a circle as $r \in \mathbb{R}$ within the context of this paper with the following attributes.

Definition 2 For any value of the radius $r \in \mathbb{R}$, the magnitude of curvature is given by $1/|r|$, and the orientation of motion on the trajectory Λ is counter-clockwise for $r > 0$ and is clockwise for $r < 0$.

We now present some useful results from [18] on the tangency of circles and the motion over trajectories formed by such tangential circles. The statements of these results have been appropriately re-phrased for the context of this paper.

Lemma 1 Any two tangential circles must satisfy the condition,

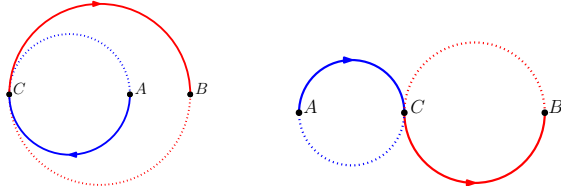
$$d(\mathbf{o}_a, \mathbf{o}_b) = |r_a - r_b| \quad (1)$$

where \mathbf{o}_a and \mathbf{o}_b are the coordinates of centres of the circles and r_a and r_b are the radii, respectively.

The relation in (1) for the distance between the centres of any two (internally or externally) tangential circles is within the context of the radius given in Definition 2.

Lemma 2 If two circles C_a and C_b are externally tangent, their radii, r_a and r_b , respectively, have opposite signs, otherwise they have the same signs.

Lemma 3 If any two circular arcs are externally tangent, then, the orientation of the motion switches from clockwise to anti-clockwise or vice-versa along the trajectory at the point of tangency. On the contrary, if the circles are internally tangent, the orientation of the motion remains the same. (Fig. 2)



(a) Internally Tangent Arcs (b) Externally Tangent Arcs

Fig. 2. Change of orientation in Internally and Externally Tangent Arcs

We know from [6] that the shortest curvature-bounded trajectory between any two oriented points A and B is either of the form Circle-Straight Line-Circle (CSC) or Circle-Circle-Circle (CCC), where C denotes a circular arc of radius r_{\min} and S denotes a straight-line segment. We denote this shortest trajectory by Λ_m and its length by l_m . There exist two types of CCC paths, namely $\{LRL, RLR\}$; and four types of CSC paths, namely $\{LSR, LSL, RSL, RSR\}$.

3 Problem Statement

Consider two points \mathbf{a} and \mathbf{b} in \mathbb{R}^2 space. Without loss of generality, we assume that the final point \mathbf{b} lies at

the origin. Let α and β be the angles that the velocity vectors make at \mathbf{a} and \mathbf{b} with respect to the positive X-axis, respectively, such that $\alpha, \beta \in [0, 2\pi)$. Using them, we define the tuples $A(\mathbf{a}, \alpha)$ and $B(\mathbf{b}, \beta)$ to be two oriented points. The objective of the paper is to construct a trajectory of any arbitrary length l_o between any two given oriented points A and B . Further, additional constraints of curvature-boundedness and minimum curvature discontinuities are imposed on the trajectory to facilitate practical implementation.

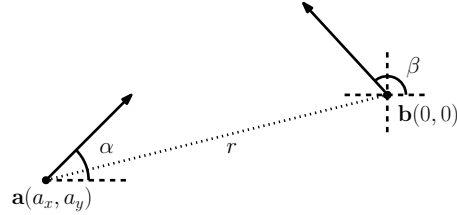


Fig. 3. Oriented points $A(\mathbf{a}, \alpha)$ and $B(\mathbf{b}, \beta)$ for trajectory design

Any feasible trajectory between A and B has five attributes to satisfy: the initial heading angle (α), the final heading angle (β), the length of the trajectory (l_o) and the relative location of points \mathbf{a} and \mathbf{b} in \mathbb{R}^2 space. To impose all of the above conditions, we design a trajectory formed by concatenating three circular arcs with exactly two pairs of circular arcs tangent to each other. We refer to such trajectories as Circle-Circle-Circle trajectories. The circles are denoted by C_1, C_2 and C_3 and their respective radii by r_1, r_2 and r_3 . In any proposed feasible trajectory,

- i. the trajectory begins at the point \mathbf{a} on C_1 ,
- ii. the circles C_1 and C_2 are tangent at a point \mathbf{c}_1 and the circles C_2 and C_3 are tangent at a point \mathbf{c}_2 . These points are called the *changeover points*.
- iii. the trajectory ends at point the \mathbf{b} on C_3 , and,
- iv. the overall trajectory is composed of the union of three circular arcs given by $\widehat{\mathbf{a}\mathbf{c}_1} \cup \widehat{\mathbf{c}_1\mathbf{c}_2} \cup \widehat{\mathbf{c}_2\mathbf{b}}$.

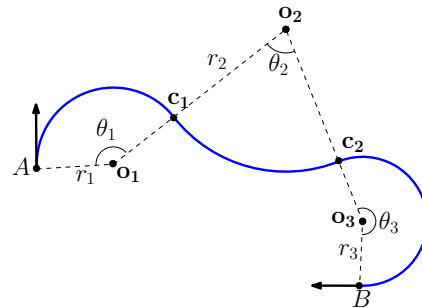


Fig. 4. Parameters of Circle-Circle-Circle Trajectory

Fig. 4 illustrates a Circle-Circle-Circle trajectory. We denote such trajectories by $C^{r_1}C^{r_2}C^{r_3}$ where r_1, r_2 and r_3 correspond to the radius of the three circles, respectively. This is a generalisation of the commonly used notation CCC which represents a Dubins Paths comprising of three

circles of curvature $1/r_{\min}$. We now highlight the motivation for using such trajectories:

- In one of our previous works [18], Circle-Circle trajectories are proposed as feasible trajectories in the given framework. The degrees of freedom of such a trajectory are exactly equal to the attributes of the desired trajectory. However, the set of reachable lengths is a subset of the maximum set of reachable lengths given by Theorem 3. We show eventually that the proposed Circle-Circle-Circle trajectories overcome this limitation.
- Three circles of varying radii lead to nine degrees of freedom in the overall trajectory. With two tangency constraints, we get seven degrees of freedom in a Circle-Circle-Circle trajectory. The extra degrees of freedom are advantageous as they lead to the existence of multiple trajectories between A and B .

The following section deals with the mathematical formulation to design $C^1C^2C^3$ trajectories between any two oriented points.

4 Existence of Circle-Circle-Circle trajectory

In this section, we explore the existence of a general $C^1C^2C^3$ trajectory while relaxing the constraint of a desired length. Then, given the oriented points $A(\mathbf{a}, \alpha)$ and $B(\mathbf{b}, \beta)$, consider the circles C_1 and C_3 . Their centres must lie on the lines normal to their respective heading vectors at the terminal points $\mathbf{a} = (a_x, a_y)$ and $\mathbf{b} = (0, 0)$. Then,

$$\mathbf{o}_1 = (a_x - r_1 \sin \alpha, a_y + r_1 \cos \alpha) \quad (2a)$$

$$\mathbf{o}_3 = (-r_3 \sin \beta, r_3 \cos \beta) \quad (2b)$$

As mentioned in Definition 2, we interpret r_1 and r_3 (and later r_2) as not just the radii of the respective circles but also the orientations of motion on them. Eqn. (2) can be viewed as the locus of the centres \mathbf{o}_1 and \mathbf{o}_3 parameterised by $r_1 \in \mathbb{R}$ and $r_3 \in \mathbb{R}$. Note that eqn. (2) holds irrespective of the choice of the intermediate curve. This implies that any curve which satisfies the the five required degrees of freedom can be used here. We choose to use a circular path so that the Dubins Shortest Path is achievable by the resulting trajectory. Depending upon the curve used, different existence conditions emerge. It is not always guaranteed that such a path will exist. Next, we proceed to find the conditions for the existence of the proposed $C^1C^2C^3$ trajectories.

4.1 Locus of the centre of circle C_2

In order to determine the conditions to check the existence of $C^1C^2C^3$ trajectories, we focus on C_2 while keeping C_1 and C_3 fixed. In other words, we assume that r_1 and r_3 take some finite values in \mathbb{R} .

Theorem 1 For any given circles C_1 and C_3 , the locus of the centre of C_2 , denoted by \mathbf{o}_2 , is a hyperbola \mathcal{H} defined by,

$$\mathcal{H} = \{\mathbf{o}_2 \in \mathbb{R}^2 \mid |d(\mathbf{o}_2, \mathbf{o}_1) - d(\mathbf{o}_2, \mathbf{o}_3)| = |r_1 - r_3|\} \quad (3)$$

where \mathbf{o}_1 and \mathbf{o}_3 are centres of C_1 and C_3 , respectively, in the feasible $C^1C^2C^3$ trajectory and r_1 and r_3 are the corresponding radii.

Proof: Let us denote the radius of C_2 as $r_2 \in \mathbb{R}$. We proceed with the proof by considering two cases:

- $r_1 r_3 > 0$: Consider $r_1 > 0$ and $r_3 > 0$. Thus, there is a left turn on both C_1 and C_3 . For this to happen, C_2 must be chosen such that the orientation of motion changes at both \mathbf{c}_1 and \mathbf{c}_2 or at neither of them. Thus, C_2 must be either externally or internally tangent to both C_1 and C_3 from Lemma 3. For internal tangency, $r_2 > 0$ from Lemma 2. Consequently, $d(\mathbf{o}_2, \mathbf{o}_1) = r_2 - r_1$ and $d(\mathbf{o}_2, \mathbf{o}_3) = r_2 - r_3$ which implies $d(\mathbf{o}_2, \mathbf{o}_1) - d(\mathbf{o}_2, \mathbf{o}_3) = r_3 - r_1$. For external tangency, $r_2 < 0$ from Lemma 2. Hence, $d(\mathbf{o}_2, \mathbf{o}_1) = r_1 - r_2$ and $d(\mathbf{o}_2, \mathbf{o}_3) = r_3 - r_2$ which implies $d(\mathbf{o}_2, \mathbf{o}_1) - d(\mathbf{o}_2, \mathbf{o}_3) = r_1 - r_3$. Combining them, we get $|d(\mathbf{o}_2, \mathbf{o}_1) - d(\mathbf{o}_2, \mathbf{o}_3)| = |r_1 - r_3|$. We get a similar relation for the case $r_1 < 0$ and $r_3 < 0$.
- $r_1 r_3 < 0$: Consider $r_1 > 0$ and $r_3 < 0$. Thus, there is a left turn on C_1 and a right turn on C_3 . For this to happen, C_2 must be chosen such that the orientation changes at exactly one point amongst \mathbf{c}_1 and \mathbf{c}_2 . From Lemma 3, C_2 must be externally tangent to one circle and internally tangent to the other. Thus, for internal tangency at C_1 and external tangency at C_3 , $r_2 > 0$ from Lemma 2. Hence, $d(\mathbf{o}_2, \mathbf{o}_1) = r_2 - r_1$ and $d(\mathbf{o}_2, \mathbf{o}_3) = r_2 - r_3$ which implies $d(\mathbf{o}_2, \mathbf{o}_1) - d(\mathbf{o}_2, \mathbf{o}_3) = r_3 - r_1$. For the other case where internal tangency occurs with C_3 and external tangency with C_1 , $r_2 < 0$ from Lemma 2. Consequently, $d(\mathbf{o}_2, \mathbf{o}_1) = r_1 - r_2$ and $d(\mathbf{o}_2, \mathbf{o}_3) = r_3 - r_2$ which implies $d(\mathbf{o}_2, \mathbf{o}_1) - d(\mathbf{o}_2, \mathbf{o}_3) = r_1 - r_3$. Combining them, we get $|d(\mathbf{o}_2, \mathbf{o}_1) - d(\mathbf{o}_2, \mathbf{o}_3)| = |r_1 - r_3|$. We get similar relation for the case $r_1 < 0$ and $r_3 > 0$.

The relation $|d(\mathbf{o}_2, \mathbf{o}_1) - d(\mathbf{o}_2, \mathbf{o}_3)| = |r_1 - r_3|$ represents the hyperbola \mathcal{H} defined in eqn. 3 whose foci are at \mathbf{o}_1 and \mathbf{o}_3 . It is depicted in Fig. 5. Hence, proved. \square

The hyperbola \mathcal{H} is important for the analysis of the existence of $C^1C^2C^3$ trajectories. For every point on \mathcal{H} , a unique $C^1C^2C^3$ trajectory exists between given A and B . We highlight some more attributes of \mathcal{H} in the following subsection.

4.2 Properties of the hyperbola \mathcal{H}

The analytical expression for \mathcal{H} is significant from theoretical as well as computational perspectives. We start the analysis with a discussion of some useful properties of \mathcal{H} .

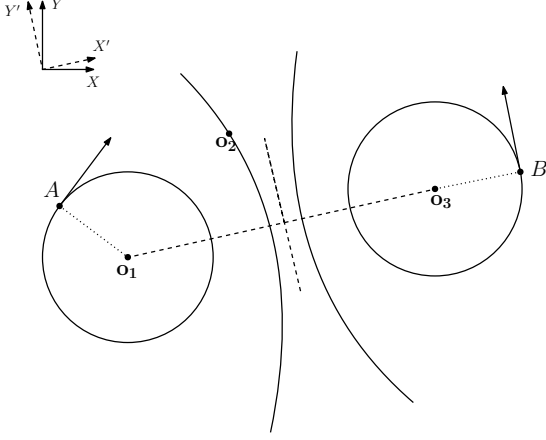


Fig. 5. Locus of \mathbf{o}_2

- The focal length and the length of the semi-major and the semi-minor axes are given by $\bar{c} = \frac{d(\mathbf{o}_3, \mathbf{o}_1)}{2}$, $\bar{a} = \frac{|r_3 - r_1|}{2}$ and $\bar{b} = \sqrt{\bar{c}^2 - \bar{a}^2}$, respectively.
- We denote the coordinate frame of reference along the semi-major and semi-minor axes as $X' - Y'$. Thereafter, we define $\hat{n} = [n_x, n_y]^T = \frac{\mathbf{o}_3 - \mathbf{o}_1}{d(\mathbf{o}_3, \mathbf{o}_1)}$ as a unit vector along the major axis. Then, $R = \begin{bmatrix} n_x & -n_y \\ n_y & n_x \end{bmatrix}$ is the rotation matrix between the frames $X - Y$ and $X' - Y'$ (see Fig. 5).
- The parametric expression of \mathcal{H} in $X' - Y'$ axis is $\mathbf{o}_2 = [a \sec k, b \tan k]^T$ where $k \in [-\pi/2, 3\pi/2)$. Through a sequence of rotation and translation the parametric coordinates of \mathbf{o}_2 in $X - Y$ coordinates are given by

$$\mathbf{o}_2 = R \begin{bmatrix} a \sec k \\ b \tan k \end{bmatrix} + \frac{\mathbf{o}_1 + \mathbf{o}_3}{2} \quad (4)$$

- Thus, all the points on \mathcal{H} can be parameterised by $k \in [-\pi/2, 3\pi/2)$. The range of k is chosen such that a continuous parameterization is achieved for each branch. The right branch is parameterised by $k \in [-\pi/2, \pi/2)$ and the left branch by $k \in [\pi/2, 3\pi/2)$.

The existence of the hyperbola is inherently related to $\{A, B\}$ and the values of $\{r_1, r_3\}$. The same is highlighted in the next result.

Theorem 2 *Given two oriented points A and B , the hyperbola \mathcal{H} exists for any r_1 and r_3 if*

$$d(\mathbf{o}_3, \mathbf{o}_1) > |r_3 - r_1|. \quad (5)$$

where \mathbf{o}_1 and \mathbf{o}_3 are given by (2).

Proof: From the definition of \mathcal{H} , we know that the length of the semi-minor axis \bar{b} is a positive real number. It then follows that $\bar{c} > \bar{a}$. This implies that $d(\mathbf{o}_3, \mathbf{o}_1) > |r_3 - r_1|$. Hence, proved. \square

Based on the proof of Theorem 2, two interesting cases arise for \mathcal{H} :

- In the limiting case of $\bar{b} = 0$, $d(\mathbf{o}_3, \mathbf{o}_1) = |r_3 - r_1|$. This is the condition for the existence of a Circle-Circle trajectory and results in the hyperbolic relation presented in [18]. Equivalently, by using appropriate values of r_1 and r_3 , a Circle-Circle trajectory can be designed within the given framework.
- If $r_1 = r_3$, then eqn. (3) reduces to two super-imposed straight lines. This line is the perpendicular bisector of the line segment joining \mathbf{o}_1 and \mathbf{o}_3 .

To summarise, given two oriented points A and B , consider the ordered pair $(r_1, r_3) \in \mathbb{R}^2$. The equation $d(\mathbf{o}_3, \mathbf{o}_1) = |r_3 - r_1|$ gives a hyperbolic relation in r_1 and r_3 which partitions the \mathbb{R}^2 space into two regions as shown in Fig. 6. Note that $(r_1, r_3) = (0, 0)$ always satisfies (5). Thus, the region highlighted in green in Fig. 6 denotes the allowed values of r_1 and r_3 to construct a feasible $\mathbf{C}^1 \mathbf{C}^2 \mathbf{C}^3$ trajectory. The boundary results in a Circle-Circle trajectory.

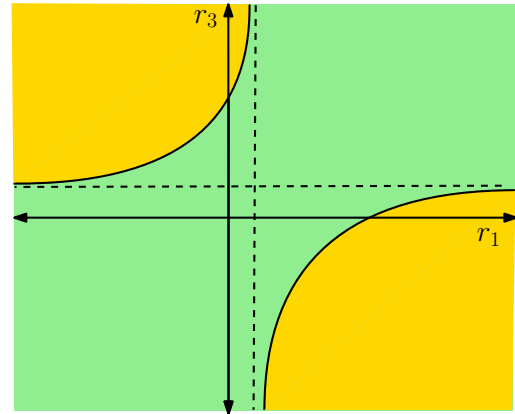


Fig. 6. Allowed values of (r_1, r_3) for the existence of $\mathbf{C}^1 \mathbf{C}^2 \mathbf{C}^3$ trajectory (in green)

The design of $\mathbf{C}^1 \mathbf{C}^2 \mathbf{C}^3$ trajectories can be effectively visualized through the variation of the three parameters $\{r_1, r_3, k\}$. Theorem 2 gives the sufficient condition for the existence of such a trajectory. Since each circle can either be a left or right turn, it follows naturally that eight permutations are possible for a $\mathbf{C}^1 \mathbf{C}^2 \mathbf{C}^3$ trajectory. Next, we proceed to classify these trajectories based on the parameters $\{r_1, r_3, k\}$.

4.3 Classification of trajectories and radius of circle \mathbf{C}_2

Any $\mathbf{C}^1 \mathbf{C}^2 \mathbf{C}^3$ trajectory can be classified into eight types: $\{LLL, RRR, LLR, RRL, LRR, RLL, LRL, RLR\}$ based upon the orientation of motion on each circular arc. The kind of tangency between any two consecutive circles, which is in turn dependent on the parameters $\{r_1, r_3, k\}$, determines the type of overall trajectory. The following results

illustrate the nature and significance of the tangency between the circles in a given $C^1C^2C^3$ trajectory.

Lemma 4 For any given r_1 and r_3 such that $r_1r_3 < 0$,

- i. if $k \in (-\pi/2, \pi/2)$, C_2 is externally tangent to C_1 and internally tangent to C_3 , and
- ii. if $k \in (\pi/2, 3\pi/2)$, C_2 is internally tangent to C_1 and externally tangent to C_3 .

Proof: Consider $r_1 > 0$ and $r_3 < 0$. We have shown in proof of Theorem 1 that for the case of internal tangency at C_1 and external tangency at C_3 , $d(\mathbf{o}_2, \mathbf{o}_1) - d(\mathbf{o}_2, \mathbf{o}_3) = r_3 - r_1 < 0$. Clearly, \mathbf{o}_2 belongs to the left branch as it is farther from \mathbf{o}_3 than \mathbf{o}_1 . For the alternate case, $d(\mathbf{o}_2, \mathbf{o}_1) - d(\mathbf{o}_2, \mathbf{o}_3) = r_1 - r_3 > 0$. This corresponds to \mathbf{o}_2 belonging to the right branch as it is farther from \mathbf{o}_1 than \mathbf{o}_3 . Thus, each branch of the hyperbola results in one particular kind of tangency for any \mathbf{o}_2 on that branch. The range of k follows automatically. We can similarly prove the case with $r_1 < 0$ and $r_3 > 0$. Hence, proved. \square

Lemma 5 For any given r_1 and r_3 such that $r_1r_3 > 0$ and $|r_1| > |r_3|$,

- i. if $k \in (-\pi/2, \pi/2)$, C_2 is externally tangent to both C_1 and C_3 , else
- ii. if $k \in (\pi/2, 3\pi/2)$, C_2 is internally tangent to both C_3 and C_1 .

For $|r_1| < |r_3|$, the branches switch.

Proof: Consider the case $r_1 > 0$ and $r_3 > 0$. We have shown in proof of Theorem 1 that for internal tangency to both C_1 and C_3 , $d(\mathbf{o}_2, \mathbf{o}_1) - d(\mathbf{o}_2, \mathbf{o}_3) = r_3 - r_1 < 0$ since $|r_1| > |r_3|$. Clearly, \mathbf{o}_2 belongs to the left branch as it is farther from \mathbf{o}_3 than \mathbf{o}_1 . For the case of external tangency, $d(\mathbf{o}_2, \mathbf{o}_1) - d(\mathbf{o}_2, \mathbf{o}_3) = r_1 - r_3 > 0$ since $|r_1| > |r_3|$. This corresponds to \mathbf{o}_2 belongs to the right branch as it is farther from \mathbf{o}_1 than \mathbf{o}_3 . If $|r_1| < |r_3|$, the branches switch. The range of k follows automatically. We can similarly prove for the case with $r_1 < 0$ and $r_3 < 0$. \square

Using Lemma 4 and Lemma 5, the classification of $C^1C^2C^3$ trajectories for various values of $\{r_1, r_3, k\}$ can be done as shown in Table 1.

Table 1
Classification of $C^1C^2C^3$ trajectories

	$k \in [-\pi/2, \pi/2)$		$k \in [\pi/2, 3\pi/2)$	
	$ r_1 \geq r_3 $	$ r_1 < r_3 $	$ r_1 \geq r_3 $	$ r_1 < r_3 $
$r_1 > 0, r_3 > 0$	LRL	LLL	LLL	LRL
$r_1 < 0, r_3 < 0$	RLR	RRR	RRR	RLR
$r_1 > 0, r_3 < 0$	LRR		LLR	
$r_1 < 0, r_3 > 0$	RLL		RRL	

Remark 1 Consider the case where, for any given A and B , only the radii of C_1 and C_2 are specified. In other words, we only have the magnitudes of r_1 and r_3 . In such a scenario, it follows from Table 1 that all eight types of the trajectories (LLL, RRR, LLR, RRL, LRR, RLL, LRL, RLR) can be constructed simply by choosing suitable signs of r_1 and r_3 .

Remark 1 highlights the existence of a trajectory of each type. The corresponding value of $r_2 \in \mathbb{R}$ for each type can be easily computed. Given any r_1 and r_2 , eqn. (4) gives the coordinates of the center of C_2 and Table 1 states the kind of tangency between C_1 and C_2 for each k . Using eqns. (2) and (1), we get the value of r_2 with appropriate signs. We derive its expression in a case-wise manner and summarise it in Table 2. Note that we define $s = d(\mathbf{o}_2, \mathbf{o}_1)$.

Table 2
Analytical expressions of r_2

	$k \in [-\pi/2, \pi/2)$		$k \in [\pi/2, 3\pi/2)$	
	$ r_1 \geq r_3 $	$ r_1 < r_3 $	$ r_1 \geq r_3 $	$ r_1 < r_3 $
$r_1 > 0, r_3 > 0$	$-s + r_1$	$s + r_1$	$s + r_1$	$-s + r_1$
$r_1 < 0, r_3 < 0$	$s + r_1$	$-s + r_1$	$-s + r_1$	$s + r_1$
$r_1 > 0, r_3 < 0$	$-s + r_1$		$s + r_1$	
$r_1 < 0, r_3 > 0$	$s + r_1$		$-s + r_1$	

The above table can be alternatively expressed compactly in the following form.

$$r_2 = \begin{cases} \text{sign}(r_1(|r_1| - |r_3|)(k - \frac{\pi}{2}))s + r_1 & , r_1r_2 > 0 \\ \text{sign}(r_1(k - \frac{\pi}{2}))s + r_1 & , r_1r_2 < 0 \end{cases} \quad (6)$$

where

$$\text{sign}(x) = \begin{cases} 1, & x \geq 0 \\ -1, & x < 0 \end{cases}$$

With the radius of the C_2 appropriately defined, the analytical expression for the two changeover points $\{\mathbf{c}_1, \mathbf{c}_2\}$ can be written as

$$\mathbf{c}_1 = \frac{r_2\mathbf{o}_1 - r_1\mathbf{o}_2}{r_2 - r_1} \quad (7a)$$

$$\mathbf{c}_2 = \frac{r_2\mathbf{o}_3 - r_3\mathbf{o}_2}{r_2 - r_3} \quad (7b)$$

Finally, we put forth an interesting observation on C_2 .

Corollary 1 For $k = \pm\frac{\pi}{2}$, C_2 limits to a straight line (a circle with infinite radius) tangent to both C_1 and C_3 .

Proof: For k tending to $\pm\pi/2$, it follows from Table 2 that s and, equivalently, $|r_2|$ tend to ∞ . Additionally, we know from Theorem 1, C_2 is always tangent to the other two circles. Thus, C_2 limits to a straight line tangent to C_1 and C_3 . Hence, proved. \square

Note that Corollary 1 states that as k tends $\pm\pi/2$, the $C^1C^2C^3$ trajectory limits to a CSC trajectory ($C^1C^{\pm\infty}C^3$ trajectory). Thus, the proposed trajectory design encapsulates all of the forms of the Dubins Shortest Paths for appropriate variation of the three circles.

The analysis of $C^1C^2C^3$ trajectories presented in this section is without any explicit constraints of a desired length of the trajectory or curvature boundedness. In the following sections, we proceed to analyse the variation of the length of the trajectory with parameters $\{r_1, r_3, k\}$ and derive the set of reachable lengths using the proposed trajectory between any pair of oriented points.

5 Variation of k for Circle-Circle-Circle trajectories

Every attribute of a Circle-Circle-Circle trajectory (like $\mathbf{c}_1, \mathbf{c}_2, r_2$, etc.) can be written as a function of the parameter k for fixed values of r_1 and r_3 . We define a function $l: [-\pi/2, 3\pi/2] \rightarrow \mathbb{R}^+$ as the length of trajectory for fixed values of r_1 and r_3 . The parameter k varies in the range $[-\pi/2, 3\pi/2]$. This variation of k can be further divided into two parts: $k \in [-\pi/2, \pi/2]$ and $k \in [\pi/2, 3\pi/2]$, i.e., over each branch of \mathcal{H} . The following interesting results then arise:

- Such a variation of k results in distinct types of $C^1C^2C^3$ trajectories for each branch of \mathcal{H} (which is discussed elaborately in Sec. 4.3).
- An infinite elongation of the trajectory can be achieved within each branch of \mathcal{H} .

We analyze the impact of these variations on the changeover points and the length of trajectory in a case-wise manner.

Case 1: $r_1r_3 > 0$

We know that for both $k = \pi/2$ and $k = -\pi/2$, C_2 becomes a common tangent line to C_1 and C_3 . These tangents, as shown in Fig. 7, divide the boundary of each circle into two parts. We label them as B_1 and B_2 as shown in Fig. 7. One of the variations in k results in C_2 being externally tangent to both C_1 and C_3 . Under such a variation, the changeover points lie in B_2 for both C_1 and C_3 as shown in Fig. 8a. The other variation results in C_2 being internally

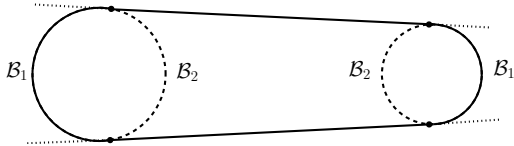


Fig. 7. Common tangents for C_1 and C_3 for $r_1r_3 > 0$

tangent to both C_1 and C_3 . The changeover points lie in B_1 for both C_1 and C_3 in such a case as shown in Fig. 8b. For both of the variations, the lengths of the $C^1C^2C^3$

trajectories tend to infinity at one end of each branch of \mathcal{H} .

Case 2: $r_1r_3 < 0$

In contrast to the previous case, the tangents, arising out $k = \pi/2$ and $k = -\pi/2$, take the form shown in Fig. 9. As before, they divide the boundary of each circle into two parts: B_1 and B_2 . The variation of k in $[-\pi/2, \pi/2]$ results in C_2 being externally tangent to C_1 and internally tangent to C_3 . Unlike the previous case, the changeover points lie in B_2 for C_1 and in B_1 for C_3 under such a variation as shown in Fig. 8c. The other variation results in C_2 being internally tangent to C_1 and externally tangent to C_3 as shown in Fig. 8d. For both of the variations, the lengths of the $C^1C^2C^3$ trajectories tend to infinity at one end of each branch of \mathcal{H} .

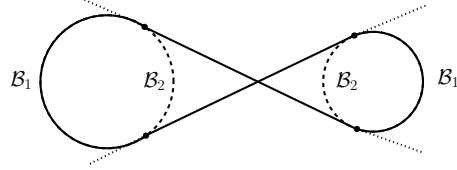


Fig. 9. Common tangents for C_1 and C_3 for $r_1r_3 < 0$

Note that while $l(k)$ goes to infinity for each variation of k , $l(k)$ is not always continuous. This is illustrated through the following result.

Lemma 6 Consider two oriented points A and B . For fixed values of $r_1, r_3 \in \mathbb{R}$, $l(\cdot)$ has at most two discontinuities. The points of discontinuity, if they exist, are at k_a and k_b where $\mathbf{c}_1(k_a) = \mathbf{a}$ and $\mathbf{c}_2(k_b) = \mathbf{b}$. Moreover, these discontinuities are jump discontinuities of magnitude $2\pi|r_1|$ at $k = k_a$ and $2\pi|r_3|$ at $k = k_b$.

Proof: For each of the variations of k , we discussed in the preceding paragraphs how \mathbf{c}_1 and \mathbf{c}_2 , i.e., the changeover points, vary continuously in either B_1 or B_2 . Let k_a and k_b be values such that $\mathbf{c}_1(k_a) = \mathbf{a}$ and $\mathbf{c}_2(k_b) = \mathbf{b}$. Consider an infinitesimal variation of k around the point $k = k_a$ and the resulting trajectories as shown in Fig. 10.

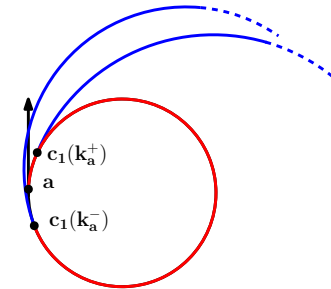


Fig. 10. Jump discontinuity in $l(\cdot)$

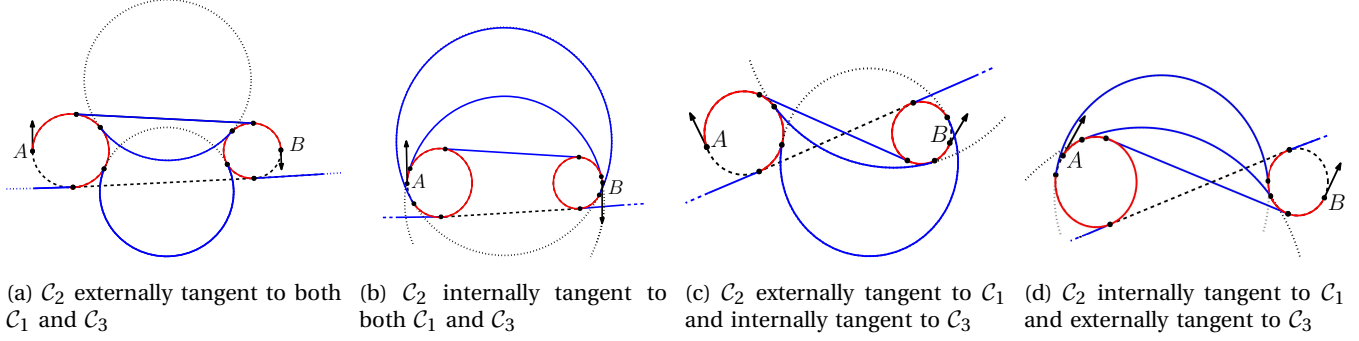


Fig. 8. Variation of C_2 in a $C^1C^2C^3$ trajectory

It is easy to see in Fig. 4 that the arc length of $\widehat{c_1c_2}$ and $\widehat{c_2b}$ is continuous along this infinitesimal variation around k_a . However, the arc length of $\widehat{ac_1}$ tends to 0 as k_a^+ tends to k_a and $\widehat{ac_1}$ tends to $2\pi|r_1|$ as k_a^- tends to k_a . Thus, $l(\cdot)$ is discontinuous at $k = k_a$. Note that in the above case, $l(k)$ jumps down by $2\pi|r_1|$ at $k = k_a$. If the location of $c_1(k_a^+)$ and $c_1(k_a^-)$ were switched, $l(k)$ would have jumped up by $2\pi|r_1|$. A similar discontinuity exists at $k = k_b$. Hence, proved. \square

It is important to note that the discontinuities at k_a and k_b need not occur simultaneously. Further, if $c_1(k)$ is not equal to \mathbf{a} and $c_b(k)$ is not equal to \mathbf{b} for any k varying over one branch of the hyperbola, we get a continuous elongation of $l(k)$ to infinity. This is true only if no curvature constraints are imposed on the trajectory. Through these results, we observe that the variation of k results in interesting properties pertaining to the length of the trajectory. We use these results along with the imposition of curvature constraint to determine the set reachable lengths between any two oriented points in the following section.

6 Curvature-bounded Circle-Circle-Circle trajectory of desired length

With important observations arising out of the variation of parameter k as discussed in the previous section, we are now able to state the set of reachable lengths. We begin the analysis with a reference to [14] for a characterisation of pairs of oriented points (A, B) based upon the kind of Dubins Shortest Path (Λ_m) between them:

$$\mathcal{O}_1 = \{(A, B) | \Lambda_m \in C_\eta S_d C_\zeta \text{ with } \eta \geq \pi\} \quad (8a)$$

$$\mathcal{O}_2 = \{(A, B) | \Lambda_m \in C_\eta S_d C_\zeta \text{ with } \zeta \geq \pi\} \quad (8b)$$

$$\mathcal{O}_3 = \{(A, B) | \Lambda_m \in C_\eta S_d C_\zeta \text{ with } d \geq 4r_{\min}\} \quad (8c)$$

$$\mathcal{O}_4 = \{(A, B) | \Lambda_m \in C_\eta S_d C_\zeta \text{ with } d(\mathbf{c}_A^r, \mathbf{c}_B^r) \geq 4r_{\min}\} \quad (8d)$$

$$\mathcal{O}_5 = \{(A, B) | \Lambda_m \in C_\eta S_d C_\zeta \text{ with } d(\mathbf{c}_A^l, \mathbf{c}_B^l) \geq 4r_{\min}\} \quad (8e)$$

where η and ζ are the arc lengths of the first and third circles, respectively, and d is the length of the straight line path. Let $\mathcal{O} := \mathcal{O}_1 \cup \mathcal{O}_2 \cup \mathcal{O}_3 \cup \mathcal{O}_4 \cup \mathcal{O}_5$ and \mathcal{O}^c be the its

complementary set

$$\mathcal{O}^c = \{(A, B) | \Lambda_m \in CSC, (A, B) \notin \mathcal{O}\}.$$

Based upon the above characterisation, the authors in [14] classify the set of reachable lengths for any two oriented points as:

Theorem 3 ([14]) Given any two oriented points A and B so that $A \neq B$, the following statements hold:

1. If $(A, B) \notin \mathcal{O} \cup \mathcal{O}^c$, for every $l_o \geq l_m$ there exists a trajectory Λ so that $l(\Lambda) = l_o$.
2. If $(A, B) \in \mathcal{O}$, for every $l_o \geq l_m$ there exists a trajectory Λ so that $l(\Lambda) = l_o$.
3. If $(A, B) \in \mathcal{O}^c$, we have that (a) for every $l_o \in [l_m, l_1] \cup [l_2, \infty)$ there exists a trajectory Λ so that $l(\Lambda) = l_o$; and (b) for any trajectory Λ we have $l(\Lambda) \notin (l_1, l_2)$.

where l_o is the length of the desired trajectory and

$$l_1 := \max\{l_{LRL}^s, l_{RLR}^s\} \quad (9a)$$

$$l_2 := \min\{l_m + 2\pi r_{\min}, l_{LRL}^l, l_{RLR}^l, \{l_{RSR}, l_{LSL}, l_{RSL}, l_{LSR}\} \setminus \{l_m\}\} \quad (9b)$$

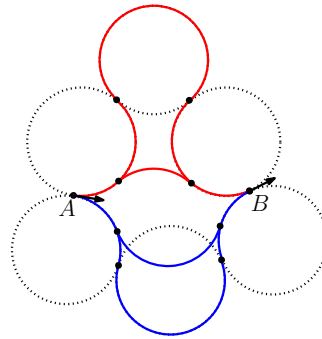


Fig. 11. Two LRL trajectories (in red) and RLR trajectories (in blue) between A and B

The various lengths of trajectory mentioned in (9) have been elaborated in [14]. For $(A, B) \in \mathcal{O}^c$, there exist two

LRL and *RLR* trajectories with the magnitude of curvature being $1/|r_{\min}|$ throughout as shown in Fig. 11 in red and blue, respectively. Note that there exists a continuous elongation between the two *LRL* (or *RLR*) trajectories if there were no curvature constraints. We denote the length of the longer *LRL* trajectory as l_{LRL}^l and the shorter one as l_{LRL}^s . The lengths l_{RLR}^l and l_{RLR}^s are defined similarly. These lengths are used to determine l_1 and l_2 in eqn. (9). Further, the following result holds for the remaining of the trajectories in eqn. (9) as shown in [14].

Lemma 7 ([14]) *If $(A, B) \in \mathcal{O}^c$, each CSC-path, with its length in $\{l_{RSR}, l_{LSL}, l_{RSL}, l_{LSR}\} \setminus \{l_m\}$, has anti-parallel tangents.*

Lemma 7 highlights that for each CSC-path, with its length in $\{l_{RSR}, l_{LSL}, l_{RSL}, l_{LSR}\} \setminus \{l_m\}$, has either $\eta \geq \pi$ or $\zeta \geq \pi$. With these observations, we present the elongation strategies for the Dubins Shortest Path to achieve a $C^1 C^2 C^3$ trajectory of a desired length between any two oriented points.

6.1 Elongation of a trajectory for $(A, B) \notin \mathcal{O} \cup \mathcal{O}^c$

The set of ordered pairs $(A, B) \notin \mathcal{O} \cup \mathcal{O}^c$ corresponds to the cases where the Dubins Shortest Path is a CCC trajectory. The following theorem illustrates the elongation strategy for such cases.

Theorem 4 *Given oriented points A and B such that $(A, B) \notin \mathcal{O} \cup \mathcal{O}^c$, there always exists a $C^1 C^2 C^3$ trajectory of any desired length $l_o \in [l_m, \infty)$.*

Proof: It is shown in [6] that if the Dubins Shortest Path

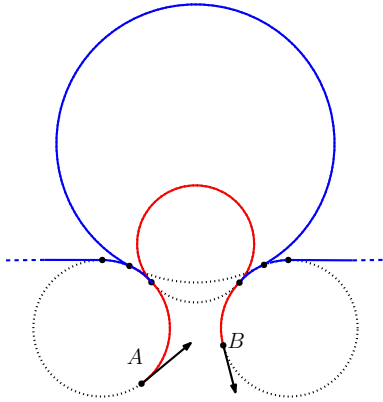


Fig. 12. Elongation of CCC Dubins Shortest Path

is of the form CCC, the arc length of the middle circle is greater than or equal to πr_{\min} . Thus, the minimum length trajectory is shown in red in Fig. 12 (for *LRL*). If we increase the magnitude of r_2 , we get a continuous elongation till infinity. We can elongate the Dubins Shortest Path of form *RLR* similarly. Hence, proved. \square

6.2 Elongation of a trajectory for $(A, B) \in \mathcal{O}$

The set \mathcal{O} is formed by the union of five different sets given by eqn. (8). We first present an important observation on this set.

Lemma 8 *For all $(A, B) \in \mathcal{O}_3$, $(A, B) \in \mathcal{O}_1 \cup \mathcal{O}_2 \cup \mathcal{O}_4 \cup \mathcal{O}_5$.*

Proof: Consider the the Dubins Shortest Path between any $(A, B) \in \mathcal{O}_3$ as a $C_\eta S_d C_\zeta$ trajectory. Clearly, if $\eta \geq \pi$ or $\zeta \geq \pi$, $(A, B) \in \mathcal{O}_1 \cup \mathcal{O}_2$. We now focus on the case of $\eta < \pi$ and $\zeta < \pi$. If the trajectory is of form *RSR*, $d(\mathbf{c}_A^r, \mathbf{c}_B^r) = d \geq 4r_{\min}$ implying $(A, B) \in \mathcal{O}_4$. Similarly, $(A, B) \in \mathcal{O}_5$ if the trajectory is of the form *LSL*.

If the trajectory is of the form *RSL*, the same has been shown in Fig. 13. Construct the normal lines at the end-points of the straight line segment (labelled as n_1 and n_2) and circle C_A^l . As $\eta < \pi$, the point \mathbf{c}_A^l lies to the left of or on the normal line n_1 . Clearly, $d(\mathbf{c}_A^l, \mathbf{c}_B^l) \geq d \geq 4r_{\min}$. Thus, $(A, B) \in \mathcal{O}_5$. Note that we can similarly show that $d(\mathbf{c}_A^r, \mathbf{c}_B^r) \geq d \geq 4r_{\min}$ and $(A, B) \in \mathcal{O}_4$ for this case. Further, the case of *LSR* path can be proven similarly. Hence, proved. \square

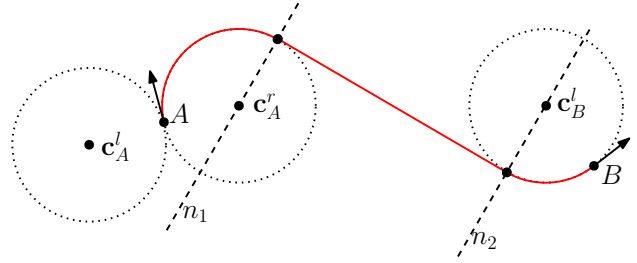


Fig. 13. For a Dubins Shortest Path of form *RSL* $d(\mathbf{c}_A^l, \mathbf{c}_B^l) \geq 4r_{\min}$

The sets given in eqn. (8) are not mutually disjoint. There exist certain pairs of (A, B) that belong to a unique set and certain pairs that belong to multiple sets. Fig. 14 illustrates a pair of oriented point that belongs to $\mathcal{O}_1 \cap \mathcal{O}_4 \cap \mathcal{O}_5$. However, Lemma 8 illustrates that \mathcal{O}_3 does not have any unique elements. Thus, it is sufficient to construct elongation strategies for the remaining four sets to explore a continuous elongation in \mathcal{O} . We analyse each of these sets separately. We begin by presenting the following result which discusses elongation strategies for set $\mathcal{O}_1 \cup \mathcal{O}_2$.

Lemma 9 *Given oriented points A and B such that $(A, B) \in \mathcal{O}_1 \cup \mathcal{O}_2$, there always exists $C^1 C^2 C^3$ trajectory of any desired length $l_o \in [l_m, \infty)$.*

Proof: We begin the proof by considering the set \mathcal{O}_1 . Thus, $\eta \geq \pi$. We divide the proof into two cases.

Case 1: Let the CSC trajectory be of form *RSR*. Clearly, $\mathbf{a} \in \mathcal{B}_2$. We continuously deform C_2 as shown in Fig. 8b. If $\mathbf{b} \in \mathcal{B}_2$, this elongation will be continuous till infinity.

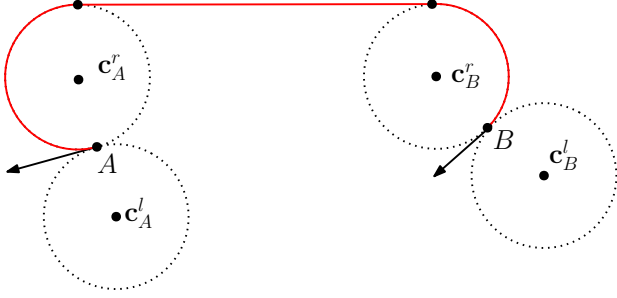


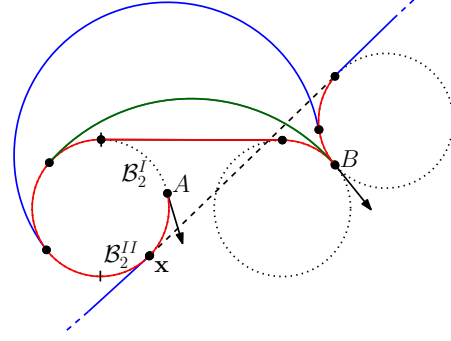
Fig. 14. CSC Dubins Shortest Path for some $(A, B) \in \mathcal{O}_1 \cap \mathcal{O}_4 \cap \mathcal{O}_5$

On the contrary, if $\mathbf{b} \in \mathcal{B}_1$, there exists a k_b such that $\mathbf{c}_2(k_b) = \mathbf{b}$. Construct circle \mathcal{C}_B^l and a transverse tangent between \mathcal{C}_1 and \mathcal{C}_B^l . This construction is shown in Fig. 15a. The point \mathbf{x} divides \mathcal{B}_2 into two arcs denoted by \mathcal{B}_2^I and \mathcal{B}_2^{II} . If $\mathbf{a} \in \mathcal{B}_2^I$, we deform \mathcal{C}_2 and get a series *RRR* trajectories until point k_b is reached as shown by a green curve in Fig. 15a. This is an *RR* trajectory. If we continue further, we will have a jump of $2\pi|r_3|$ as discussed in Lemma 6. To ascertain a continuous elongation of the length of the trajectory, we proceed to deform \mathcal{C}_2 such that it is internally tangent to \mathcal{C}_1 and externally to \mathcal{C}_B^l as shown in blue in Fig. 15a resulting in a *RRL* trajectory. Since $\mathbf{a} \in \mathcal{B}_2^I$, we will have a continuous elongation until $|r_2|$ goes to infinity as shown in Fig. 15a.

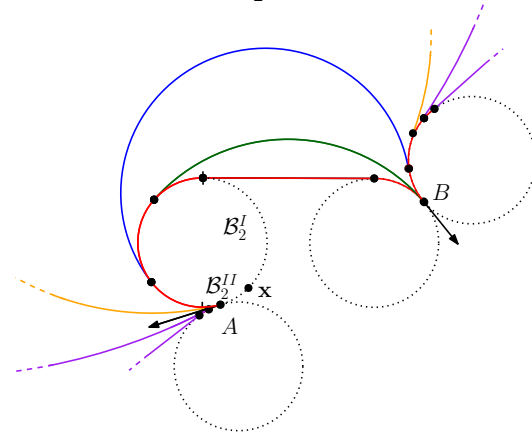
If $\mathbf{a} \in \mathcal{B}_2^{II}$, construct \mathcal{C}_A^l . We deform \mathcal{C}_2 similarly as in the previous case until the point k_a is reached such that $\mathbf{c}_1(k_a) = \mathbf{a}$ before the length of trajectory goes to infinity. This is an *RL* trajectory as shown by the yellow curve in Fig. 15b. If we proceed similarly, we get a jump discontinuity of $2\pi|r_1|$. Instead, we now deform \mathcal{C}_2 such that it is externally tangent to both \mathcal{C}_A^l and \mathcal{C}_B^l resulting in *LRL* trajectories and a continuous deformation after $k = k_a$ until the length reaches infinity. Note that in all the cases, $|r_2| \geq r_{\min}$. Thus, the curvature constraint on the trajectory is not violated. We can similarly achieve a continuous elongation of an *LSL* path with $\eta \geq \pi$.

Case 2: Let the *CSC* trajectory be of form *RSL*. For $\eta \geq \pi$, \mathbf{a} can lie in either \mathcal{B}_1 or \mathcal{B}_2 . If $\mathbf{a} \in \mathcal{B}_2$, we deform \mathcal{C}_2 as shown in Fig. 8d such that $\mathbf{c}_1 \neq \mathbf{a}$ always. Further, if $\mathbf{b} \in \mathcal{B}_1$, we get a continuous elongation as $\mathbf{c}_2 \in \mathcal{B}_2$ and no jump discontinuity is encountered. If $\mathbf{b} \in \mathcal{B}_2$, there exist a k_b such that $\mathbf{c}_2(k_b) = \mathbf{b}$. However, there is a jump down discontinuity and the set of reachable lengths is given by $l \in [l_m, l_b + 2\pi|r_3|) \cup [l_b, \infty) = [l_m, \infty)$ where $l(k_b) = l_b$. Thus, a continuous elongation of the trajectory exists until its length goes to infinity.

If $\mathbf{a} \in \mathcal{B}_1$, we again proceed in a case-wise manner. If $\mathbf{b} \in \mathcal{B}_2$, we deform \mathcal{C}_2 as shown in Fig. 8c. For such a variation, $\mathbf{c}_1 \in \mathcal{B}_2$ and $\mathbf{c}_2 \in \mathcal{B}_1$ resulting in no jump discontinuities and we get a continuous elongation of the trajectory till infinity. If $\mathbf{b} \in \mathcal{B}_1$, we proceed in a similar manner as the case of $\mathbf{a} \in \mathcal{B}_2^{II}$ in Case 1. The same has been highlighted in



(a) $\mathbf{a} \in \mathcal{B}_2^I$ and $\mathbf{b} \in \mathcal{B}_1$



(b) $\mathbf{a} \in \mathcal{B}_2^{II}$ and $\mathbf{b} \in \mathcal{B}_1$

Fig. 15. Elongation of $C_\eta S_d C_\chi$ trajectory with $\eta \geq \pi$

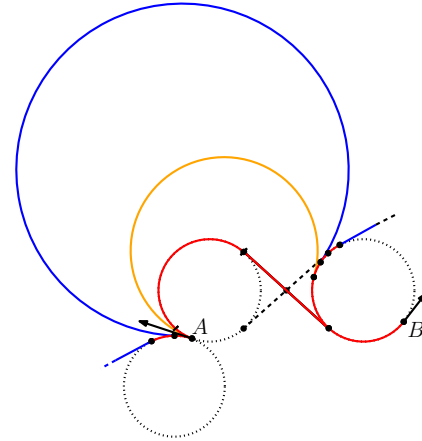


Fig. 16. Elongation of *RSL* trajectory with $\eta \geq \pi$ where $\mathbf{a} \in \mathcal{B}_1$ and $\mathbf{b} \in \mathcal{B}_1$

Fig. 16. We can similarly achieve a continuous elongation for an *LSR* path.

The elongation strategies mentioned here can be similarly applied to the cases where $\zeta \geq \pi$, i.e., $(A, B) \in \mathcal{O}_2$. Thus, a continuous elongation of trajectory exist using $C^{r_1} C^{r_2} C^{r_3}$ trajectory for all $(A, B) \in \mathcal{O}_1 \cup \mathcal{O}_2$. Hence, proved. \square

An important idea emerges from the proof of Lemma 9. The deformation of C_2 is realised by the variation of the parameter k . If the point k_a (or k_b), defined in Lemma 6, is reached in this deformation, one should switch C_1 (or C_3) from C_A^l to C_A^r or vice-versa (or C_B^l to C_B^r or vice-versa) for further deformation of C_2 instead of proceeding on the same circle. The arc length of $\widehat{ac_1}$ (or $\widehat{c_2b}$) goes to zero as k_a (or k_b) is approached and starts increasing after the switch, preserving its continuity and, in turn, the continuity of the overall length of trajectory (see Fig. 17). The switching of the terminal circles can be alternatively viewed as changing r_1 (or r_3) from r_{\min} to $-r_{\min}$ or vice versa.

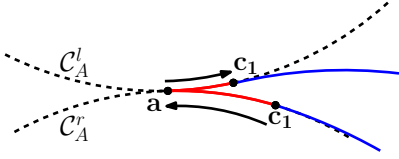


Fig. 17. Continuous elongation of $C^1 C^2 C^3$ trajectory

We now discuss the set $\mathcal{O}_4 \cup \mathcal{O}_5$. Clearly, any pair $(A, B) \in \mathcal{O}_4 \cup \mathcal{O}_5$ such that $\eta \geq \pi$ or $\zeta \geq \pi$ can be elongated continuously to infinitely large lengths from Lemma 9. We analyse the remaining cases in the following result.

Lemma 10 *Given oriented points A and B such that $(A, B) \in \mathcal{O}_4 \cup \mathcal{O}_5$ with $\eta < \pi$ and $\zeta < \pi$, there always exists a $C^1 C^2 C^3$ trajectory of any desired length $l_o \in [l_m, \infty)$.*

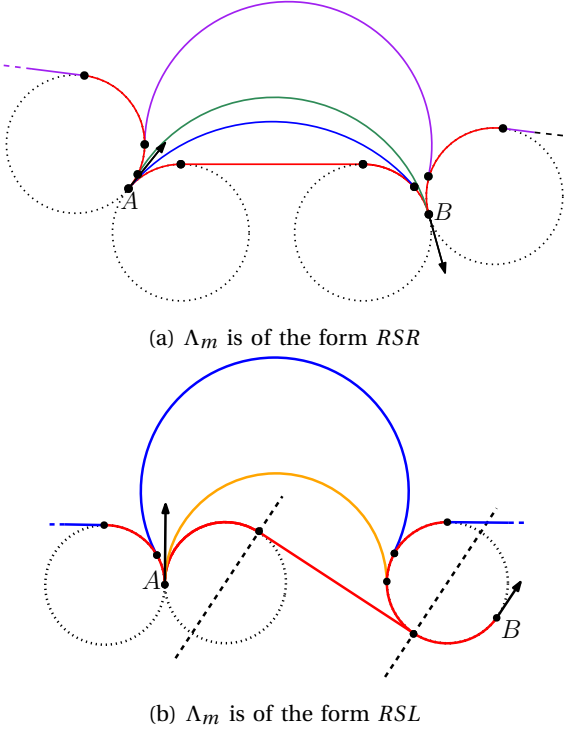


Fig. 18. Elongation of $C^1 S_d C^2$ trajectory with $d(c_A^l, c_B^l) \geq 4r_{\min}$

Proof: The proof is similar to that of Lemma 9. It can be

illustrated for different cases of RSR and RSL trajectories through Fig. 18. \square

The following theorem follows from Lemma 9 and 10.

Theorem 5 *Given oriented points A and B such that $(A, B) \in \mathcal{O}$, there exists $C^1 C^2 C^3$ trajectory for all lengths $l_o \in [l_m, \infty)$.*

6.3 Elongation of trajectory for $(A, B) \in \mathcal{O}^c$

For all $(A, B) \in \mathcal{O}^c$, there exist trajectories of lengths l_{LRL}^s and l_{RLR}^s as shown in Fig. 11. Using the definitions of l_1 and l_2 from (9), the following result illustrates the elongation strategy for such cases.

Theorem 6 *Given oriented points A and B such that $(A, B) \in \mathcal{O}^c$, there always exists a $C^1 C^2 C^3$ trajectory of any desired length $l_o \in [l_m, l_1] \cup [l_2, \infty)$ where l_1 and l_2 are given by eqn. (9).*

Proof: Consider the trajectories whose lengths are mentioned in (9). Without loss of generality, let $l_1 = l_{RLR}^s$. Fig. 19 shows the elongation strategy for an LSL minimum path. We deform C_2 resulting in a series of LLL trajectories until point k_a is reached. This trajectory is of the type LL . To preserve the continuity of elongation, we construct C_2 between C_A^r and C_3 resulting in a series of RLL trajectories until a point k_b is reached. Henceforth, C_2 is constructed such that it is externally tangent to C_A^r and C_B^r forming a series of RRL trajectories. This C_2 is deformed until we get a trajectory whose length is l_{RLR}^s . Thus, a $C^1 C^2 C^3$ trajectory exists for every $l_o \in [l_m, l_1]$. Note that it might happen that k_b is reached earlier than k_a . In such a case, C_3 is switched first. The proof follows similarly.

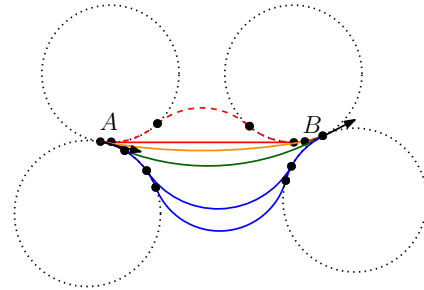


Fig. 19. Elongation of trajectory from l_m to l_1 when $(A, B) \in \mathcal{O}^c$

Clearly, trajectories of length $\{l_{RLR}^l, l_{LRL}^l\}$ have arc lengths of C_2 greater than πr_{\min} as shown in Fig. 11. These can be continuously elongated till infinity using strategies in Theorem 4. Further, we know from Lemma 7 that the trajectories of lengths $\{l_{RSR}, l_{LSL}, l_{RSL}, l_{LSR}\} \setminus \{l_m\}$ have either $\eta \geq \pi$ or $\zeta \geq \pi$. Thus, they can also be elongated continuously using Lemma 9. Lastly, the trajectory of length $l_m + 2\pi r_{\min}$ can also be continuously elongated till infinity using Lemma 9. Consequently, there exists a $C^1 C^2 C^3$ trajectory for all $l_o \in [l_2, \infty)$. Hence proved. \square

Theorems 4 - 6 show that the proposed $C^1 C^2 C^3$ trajectories can form curvature-bounded trajectories of any desired lengths. The corresponding set of reachable lengths is exactly the same as the maximum reachability set mentioned in Theorem 3 for all pairs of oriented points (A, B) . Further, the proposed strategies guarantee a maximum of two changeover points in the entire trajectory between A and B for any desired length.

The analysis of the set of reachable lengths till now is done with the values of r_1 and r_3 fixed. They took the value of $\pm r_{\min}$ depending upon the kind of Dubins Shortest Path between (A, B) and the subsequent elongation strategy. We have established that the maximum reachability set is completely covered with just these values of r_1 and r_3 for the $C^1 C^2 C^3$ trajectory. Next, we proceed to discuss the variation of r_1 and r_3 values and its implication on the lengths of the $C^1 C^2 C^3$ trajectories.

6.4 Variation of r_1 and r_3 for Circle-Circle-Circle trajectories

The design of a Circle-Circle-Circle trajectory is accomplished by a suitable variation of $\{r_1, r_3, k\}$. All the reachable lengths are achieved by varying k in $[-\pi/2, 3\pi/2)$ and r_1 and r_3 in $\{-r_{\min}, r_{\min}\}$. In this section, we explore the effect of a continuous variation of r_1 and r_3 in $\mathbb{R} \setminus (-r_{\min}, r_{\min})$. Given a desired length l_o , we show that this results in the existence of multiple trajectories between the oriented points A and B . We begin the analysis with the following definition of a trajectory $\tilde{\Lambda}$.

Definition 3 Given two oriented points A and B , consider that the radii r_1 and r_3 take some fixed values in \mathbb{R} such that eqn. (5) holds. Let

$$\tilde{l} = \min_{k \in [-\pi/2, 3\pi/2)} l(k)$$

be the length of the shortest trajectory in this framework. We denote this trajectory by $\tilde{\Lambda}$.

The trajectory $\tilde{\Lambda}$ can be found numerically by iterating over $k \in [-\pi/2, 3\pi/2)$. Note that it can be a CSC trajectory which is a $C^1 C^2 C^3$ trajectory with $|r_2|$ tending to infinity. We should highlight that for appropriate values of (A, B, r_1, r_3) with $r_1, r_3 \in \{\pm r_{\min}\}$, $\tilde{\Lambda} = \Lambda_m$. We define the following sets based upon the trajectory $\tilde{\Lambda}$.

$$\begin{aligned} \mathcal{P}_0 &= \{(A, B, r_1, r_3) | \tilde{\Lambda} \in C_\eta^{r_1} C_\mu^{r_2} C_\zeta^{r_3} \text{ with } \mu \geq \pi|r_2|\} \\ \mathcal{P}_1 &= \{(A, B, r_1, r_3) | \tilde{\Lambda} \in C_\eta^{r_1} C_\mu^{r_2} C_\zeta^{r_3} \text{ with } \eta \geq \pi|r_1|\} \\ \mathcal{P}_2 &= \{(A, B, r_1, r_3) | \tilde{\Lambda} \in C_\eta^{r_1} C_\mu^{r_2} C_\zeta^{r_3} \text{ with } \zeta \geq \pi|r_3|\} \\ \mathcal{P}_3 &= \{(A, B, r_1, r_3) | \tilde{\Lambda} \in C_\eta^{r_1} C_\mu^{r_2} C_\zeta^{r_3} \text{ with} \\ &\quad d(\mathbf{c}_A^r, \mathbf{c}_B^r) \geq |r_1| + |r_3| + 2r_{\min}\} \\ \mathcal{P}_4 &= \{(A, B, r_1, r_3) | \tilde{\Lambda} \in C_\eta^{r_1} C_\mu^{r_2} C_\zeta^{r_3} \text{ with} \\ &\quad d(\mathbf{c}_A^l, \mathbf{c}_B^l) \geq |r_1| + |r_3| + 2r_{\min}\} \end{aligned}$$

where η , μ and ζ are arc lengths of the three circles, respectively. The points \mathbf{c}_A^r and \mathbf{c}_A^l are the centres of the circles of radius $|r_1|$ at A corresponding to right and left turns, respectively. The points \mathbf{c}_B^r and \mathbf{c}_B^l are the centres of the circles of radius $|r_3|$ at B corresponding to right and left turns, respectively. We define the set $\mathcal{P} := \mathcal{P}_1 \cup \mathcal{P}_2 \cup \mathcal{P}_3 \cup \mathcal{P}_4$. The set \mathcal{P} is a generalisation of the set \mathcal{O} for different values of r_1 and r_3 . The following theorem states the set of reachable lengths for these sets.

Theorem 7 Given two oriented points A and B , consider that the radii r_1 and r_3 take some fixed values in \mathbb{R} such that eqn. (5) holds. If $(A, B, r_1, r_3) \in \mathcal{P}_0 \cup \mathcal{P}$, then there exists a $C^1 C^2 C^3$ trajectory for all desired lengths $l_o \in [\tilde{l}, \infty)$.

Proof: The proof for the sets \mathcal{P}_0 and \mathcal{P} is similar to that of Theorems 4 and 5, respectively. \square

This concludes our discussion on the set of reachable lengths for curvature-bounded trajectories of desired lengths. Theorem 7 provides set of reachable lengths for any given values of r_1 and r_3 in \mathbb{R} through the construction of sets \mathcal{P}_0 and \mathcal{P} .

Remark 2 It should be noted that the reachability set in Theorem 7 is always a subset of the maximum set of reachable lengths. Thus, it illustrates the existence of multiple trajectories for the same desired length. Note that this is in contrast to the results presented in Theorems 4 - 6 which prove the existence of at least one $C^1 C^2 C^3$ trajectory of a reachable desired length. Further, all of the proposed elongation strategies result in curvature-bounded trajectories with at most two curvature discontinuities.

7 Numerical simulations

In this section, we illustrate the results presented in this paper through the following numerical simulations.

Example 1: Consider $A = (-3m, 1m, 0.785rad)$ and $B = (0m, 0m, 0rad)$. The Dubins Shortest Path between A and B for $r_{\min} = 1m$ is an RSL path of length $l_m = 3.484m$. The given $(A, B) \in \mathcal{O}^c$ with $l_1 = 4.144m$ and $l_2 = 6.856m$ from eqn. (9). Consequently, the set of reachable lengths can be defined. We seek to construct trajectories of lengths $l_o \in \{3.60m, 4.05m, 7.00m, 11.15m, 12.45m, 14.90m\}$. Table 3 shows the computed values of r_2 . Fig. 20 shows the various feasible trajectories. The Dubins Shortest Path has been highlighted in red.

Example 2: Consider $A = (-30m, 10m, 0.714rad)$ and $B = (0m, 0m, 0rad)$. The Dubins Shortest Path for $r_{\min} = 1m$ is an RSL path of length $l_m = 31.809m$. The given $(A, B) \in \mathcal{O}_3$. Thus, a $C^1 C^2 C^3$ trajectory exists for all $l_o \in [l_m, \infty)$. We seek to construct trajectories of length $l = 44.5m > l_m$. There exists infinitely many such trajectories between A and B . We arbitrarily choose r_1 and r_3 values and check if

Table 3
Computed values of r_2 for trajectories between A and B of various lengths

$l_0(m)$	$r_1(m)$	$r_2(m)$	k	$r_3(m)$	Label
3.484	-1.00	∞	$\pi/2$	1.00	—
3.60	-1.00	-1.37	2.634	1.00	—
4.05	1.00	-1.031	-0.379	1.00	—
7.00	1.00	-1.015	0.360	1.00	—
11.15	1.00	-1.57	0.748	1.00	—
12.45	-1.00	1.49	-0.634	1.00	—
14.90	-1.00	1.87	-0.876	1.00	—

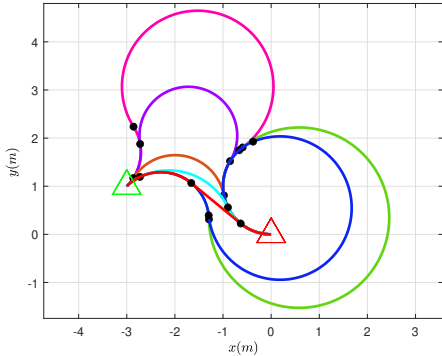


Fig. 20. Trajectories between $A = (-3m, 1m, 0.785rad)$ and $B = (0m, 0m, 0rad)$ of various lengths with changeover points labeled (\bullet)

$(A, B, r_1, r_3) \in \mathcal{P}_0 \cup \mathcal{P}$. If $l_0 \geq \tilde{l}$, then we proceed to compute the values of r_2 . Table 4 shows the computed values of \tilde{l} and r_2 . Fig. 21 shows the simulated trajectories in the \mathbb{R}^2 plane. Note that for the trajectory in green, r_1 and r_3 values are appropriately chosen such that we don't require three circular arcs resulting in a LL trajectory.

Table 4
Computed values of r_2 and k for trajectories between A and B of length $l_0 = 44.5m$

$r_1(m)$	$r_3(m)$	$\tilde{l}(m)$	$r_2(m)$	k	Label
-2.500	1.500	32.099	20.683	0.805	—
-5.500	-3.580	33.467	9.601	0.167	—
-1.000	-1.010	32.389	14.798	3.328	—
13.790	10.010	35.998	-9.145	-0.242	—
1.940	12.010	35.673	-27.42	2.029	—
2.040	59.314	N/A	N/A	N/A	—

8 Conclusion

In this paper, our objective is to construct curvature-bounded trajectories of any desired length between any two given oriented points. To do so, we propose to design the trajectory utilising three circular arcs of varying radii for the same, referred to as a Circle-Circle-Circle ($C^{r_1}C^{r_2}C^{r_3}$) trajectory. The feasible trajectory is constructed by first fixing the terminal circles. Then, we show that the locus of the centre of C_2 is a hyperbola \mathcal{H}

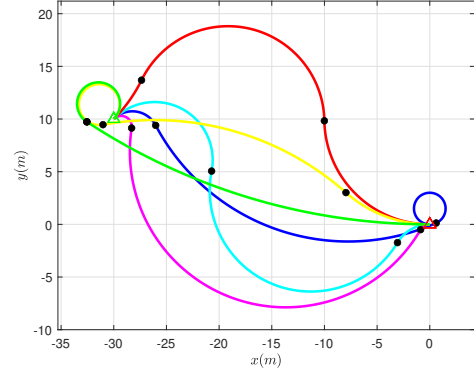


Fig. 21. Trajectories between A and B of length $l_0 = 44.5m$ with changeover points labeled (\bullet)

parameterised by the argument k . The overall trajectory is then defined using the three parameters: the radii of the terminal circles $\{r_1, r_3\}$ and an argument k . In the absence of any constraints on the length of the trajectory, we derive the necessary conditions for the existence of $C^{r_1}C^{r_2}C^{r_3}$ trajectories. Now, such trajectories can be of eight types: $\{LLL, LLR, LRR, LRL, RRL, RLL, RLR, RRR\}$. We also present a complete classification of the trajectories into these forms based upon the values of $\{r_1, r_3, k\}$.

In the presence of curvature boundedness, we propose to elongate the circular arcs C^{r_i} , $i \in \{1, 2, 3\}$ to achieve trajectories of desired lengths. In this regard, we show that the argument k is critical as its variation, divided over the two branches of the hyperbola, results in an infinite (not necessarily continuous) elongation of the trajectory. However, this variation leads to jump discontinuities in the length of the trajectory for some configurations of (A, B) . To resolve this issue, we propose elongation strategies which guarantee the existence of curvature-bounded trajectories of any desired length for any configuration (A, B) . Further, we show that the set of reachable lengths is exactly equal to that proposed in [14] guaranteeing maximum coverage of the reachability set. In addition to this, the proposed elongation strategies also lead to the existence of multiple trajectories of desired lengths simply through the variation of r_1 and r_3 .

The paper concludes with numerical solutions illustrating and validating various results discussed in the paper. Future works in this direction may extend this approach to trajectory planning in the presence of obstacles. Further, additional constraints like minimum control effort maybe imposed as the trajectory is under-constrained for the problem addressed in this paper.

References

[1] H. Vorobieva, S. Glaser, N. Minoiu-Enache, and S. Mammar, "Automatic parallel parking in tiny spots: Path planning and control," *IEEE Transactions on Intelligent Transportation Systems*, vol. 16, no. 1, pp. 396–410, 2014.

- [2] A. Bolu and Ö. Korçak, "Path planning for multiple mobile robots in smart warehouse," in *2019 7th International Conference on Control, Mechatronics and Automation (ICCM)*, pp. 144–150, IEEE, 2019.
- [3] L. Cheng, H. Lu, T. Lei, and J. Chen, "Path planning for anti-ship missile using tangent based dubins path," in *2019 2nd International Conference on Intelligent Autonomous Systems (ICoIAS)*, pp. 175–180, IEEE, 2019.
- [4] C. Schumacher, P. Chandler, S. Rasmussen, and D. Walker, "Path elongation for uav task assignment," in *ALAA Guidance, Navigation, and Control Conference and Exhibit*, p. 5585, 2003.
- [5] J. Cao, J. Cao, Z. Zeng, B. Yao, and L. Lian, "Toward optimal rendezvous of multiple underwater gliders: 3d path planning with combined sawtooth and spiral motion," *Journal of Intelligent & Robotic Systems*, vol. 85, pp. 189–206, 2017.
- [6] L. E. Dubins, "On curves of minimal length with a constraint on average curvature, and with prescribed initial and terminal positions and tangents," *American Journal of mathematics*, vol. 79, no. 3, pp. 497–516, 1957.
- [7] J.-D. Boissonnat, A. Cérézo, and J. Leblond, "Shortest paths of bounded curvature in the plane," *Journal of Intelligent and Robotic Systems*, vol. 11, pp. 5–20, 1994.
- [8] X.-N. Bui and J.-D. Boissonnat, *Accessibility region for a car that only moves forwards along optimal paths*. PhD thesis, INRIA, 1994.
- [9] Y. Meyer, P. Isaiiah, and T. Shima, "On dubins paths to intercept a moving target," *Automatica*, vol. 53, pp. 256–263, 2015.
- [10] Y. Ding, B. Xin, and J. Chen, "Curvature-constrained path elongation with expected length for dubins vehicle," *Automatica*, vol. 108, p. 108495, 2019.
- [11] M. Shanmugavel, A. Tsourdos, R. Zbikowski, and B. White, "Path planning of multiple uavs using dubins sets," in *AIAA Guidance, Navigation, and Control Conference and Exhibit*, p. 5827, 2005.
- [12] A. Ortiz, D. Kingston, and C. Langbort, "Multi-uav velocity and trajectory scheduling strategies for target classification by a single human operator," *Journal of Intelligent & Robotic Systems*, vol. 70, pp. 255–274, 2013.
- [13] M. Shanmugavel, A. Tsourdos, B. White, and R. Zbikowski, "Co-operative path planning of multiple uavs using dubins paths with clothoid arcs," *Control engineering practice*, vol. 18, no. 9, pp. 1084–1092, 2010.
- [14] Z. Chen, K. Wang, and H. Shi, "Elongation of curvature-bounded path," *Automatica*, vol. 151, p. 110936, 2023.
- [15] H. Chitsaz and S. M. LaValle, "Time-optimal paths for a dubins airplane," in *2007 46th IEEE conference on decision and control*, pp. 2379–2384, IEEE, 2007.
- [16] V. Patsko and A. Fedotov, "Three-dimensional reachable set for the dubins car: Foundation of analytical description," *Communications in Optimization Theory*, pp. 1–42, 2022.
- [17] V. Patsko and A. Fedotov, "Three-dimensional reachability set for a dubins car: Reduction of the general case of rotation constraints to the canonical case," *Journal of Computer and Systems Sciences International*, vol. 62, no. 3, pp. 445–468, 2023.
- [18] A. K. Rao, K. P. Singh, and T. Tripathy, "Curvature bounded trajectories of desired lengths for a dubins vehicle," *Automatica*, vol. 167, p. 111749, 2024.
- [19] R. Livermore, R. Tsalik, and T. Shima, "Elliptic guidance," *Journal of Guidance, Control, and Dynamics*, vol. 41, no. 11, pp. 2435–2444, 2018.
- [20] M. Gun-Hee, S.-W. Shim, and T. Min-Jea, "Bezier-curve navigation guidance for impact time and angle control," *INCAS BULLETIN*, vol. 10, pp. 105–115, 03 2018.
- [21] W. L. Xu, B. L. Ma, and S. K. Tso, "Curve fitting approach to motion planning of nonholonomic chained systems," in *Proceedings 1999 IEEE International Conference on Robotics and Automation (Cat. No. 99CH36288C)*, vol. 1, pp. 811–816, IEEE, 1999.
- [22] I.-S. Jeon, J.-I. Lee, and M.-J. Tahk, "Impact-time-control guidance with generalized proportional navigation based on nonlinear formulation," *Journal of Guidance, Control, and Dynamics*, vol. 39, no. 8, pp. 1885–1890, 2016.
- [23] X. Chen and J. Wang, "Optimal control based guidance law to control both impact time and impact angle," *Aerospace Science and Technology*, vol. 84, pp. 454–463, 2019.
- [24] W. Yao, N. Qi, J. Zhao, and N. Wan, "Bounded curvature path planning with expected length for dubins vehicle entering target manifold," *Robotics and Autonomous Systems*, vol. 97, pp. 217–229, 2017.